Research Article

Guorui Zhang, Laicong Liao, Peijie Liu, Jianhua Ren and Yuan Ruan*

MicroRNA-766-3p modulates the progression of delayed fracture healing by targeting *TGFBR1*

https://doi.org/10.1515/tjb-2025-0212
Received May 22, 2025; accepted August 6, 2025;
published online August 26, 2025

Abstract

Objectives: A certain number of patients frequently encounter delayed fracture healing (DFH) following surgery. This study intended to investigate the functionality of miR-766-3p in the progression of DFH.
Methods: The research encompassed 100 normal tibial fracture healing patients and 95 DFH patients. RT-qPCR was implemented to measure the expression, and the ROC was used to determine the diagnostic value of miR-766-3p for DFH patients. Cox regression was performed to identify the independent risk factors associated with DFH. Moreover, we further analyzed the regulatory effects of miR-766-3p and *TGFBR1* on osteogenic markers. The CCK-8 method and flow cytometry were utilized to detect proliferation and apoptosis. The levels of tumor necrosis factor-alpha (TNF-α) and interleukin-6 (IL-6) were quantified using enzyme-linked immunosorbent assay (ELISA). The dual-luciferase reporter gene assay was carried out to detect the targeted relationship.
Results: In DFH patients, miR-766-3p exhibited a downward movement. miR-766-3p served as an independent prognostic factor influencing DFH. miR-766-3p increased after the induction and differentiation of MC3T3-E1 cells. Elevated miR-766-3p could enhance the expression of osteogenic markers, facilitate proliferation and differentiation, inhibit inflammatory reactions, and reduce apoptosis. Additionally, when *TGFBR1* was upregulated, it reversed the effect of miR-766-3p on osteoblasts. miR-766-3p may emerge as a feasible predictive biomarker for patients with DFH.
Conclusions: miR-766-3p exerted its regulatory function on DFH by targeting *TGFBR1*.

Keywords: DFH; miR-766-3p; *TGFBR1*; proliferation

Introduction

Globally, fractures represent a relatively common condition, with an annual incidence rate ranging from 0.25 to 0.38 % [1, 2]. Surgery constitutes an important approach for treating traumatic fractures. However, a certain number of patients frequently encounter delayed fracture healing following surgery, which elevates the risk of refracture and non-union and has a severe impact on the prognosis of patients [3]. After the healing of the majority of fractures, their structure and bone function can fully return to normal. Nevertheless, there are still some fracture patients who ultimately experience abnormal healing, which may result in a prolonged disease course [4]. Studies have indicated that imbalances in the inflammatory response may lead to DFH [5]. Hence, exploring serum markers that can predict DFH holds great significance for guiding timely clinical intervention and treatment and thereby enhancing the prognosis of patients.

MicroRNAs (miRNAs) exert significant roles in crucial cellular processes [6–8]. Among them, miR-146a/b has been confirmed to modulate *FGF2* [9]. In the serum of fracture patients, it has been discovered that miR-21, miR-23a, and miR-24 are upregulated [10]. It should be noted that miR-766-3p can not only function as a biomarker for the treatment of colon cancer [11] but also participate in the regulation of various pathological processes. It is related to the regulation of the extracellular matrix, injury response, inflammatory

Guorui Zhang and Laicong Liao should be considered joint first author.

***Corresponding author: Yuan Ruan**, Department of Orthopedics, Huanggang Central Hospital, No. 6, Qi'an Avenue, Huangzhou District, Huanggang City, 438000, Hubei Province, China, E-mail: Ruanyuan198708@163.com. https://orcid.org/0009-0005-7798-6634
Guorui Zhang, Department of Orthopedics, Guyuan People's Hospital, Guyuan, China. https://orcid.org/0009-0001-3852-6775
Laicong Liao, Orthopedics and Rehabilitation, University of Dundee, Scotland, UK. https://orcid.org/0009-0006-6763-7032
Peijie Liu and Jianhua Ren, Second Department of Orthopaedics, Cangxian Hospital, Cangzhou, China. https://orcid.org/0009-0004-0239-5082 (P. Liu)

response, and cell apoptosis, and also participates in intervertebral disc degeneration [12]. Additionally, studies have indicated that miR-766-3p is positively related to the bone mineral density (BMD) value of osteoporosis patients [13], and miR-766-3p overexpression can inhibit chondrocyte apoptosis [14]. Moreover, the study found that miR-766-3p inhibits the triggering of nuclear factor-κB induced by cytokines [15]. However, at present, miR-766-3p in the regulation of DFH remains unclear.

TGFBR1 plays a crucial role in bone regeneration [16]. Prior studies have demonstrated that dexmedetomidine enhances the expression of *TGFBR1* in mouse bone marrow mesenchymal stem cells, thereby influencing osteogenic differentiation [17]. *TGFBR1* is implicated in osteoblast differentiation and bone formation [18], and its inhibition significantly promotes the differentiation capacity of mouse osteoblasts [19]. Furthermore, bioinformatics analysis revealed that *TGFBR1* was a downstream target gene of miR-766-3p. Therefore, we hypothesized that miR-766-3p/*TGFBR1* may be involved in the regulation of mechanisms related to DFH.

In summary, by analyzing the impact of miR-766-3p on the prognosis of DFH and integrating findings from relevant cell experiments, we thoroughly investigated the specific mechanism underlying the miR-766-3p/*TGFBR1* axis in DFH. This study aimed to provide a novel theoretical foundation for further research on DFH.

Materials and methods

Study population

This study was approved by the Cangxian Hospital Ethics Committee (approval number: 2,021,003, Date: 2021.01.11), and the subjects signed the informed consent form. All procedures adhere to the Helsinki Declaration.

195 fracture patients who underwent fixation treatment at Cangxian Hospital between January 2021 and October 2023 were included in this study. The 195 fracture patients included in the study were followed up every two weeks for three months. Patients who successfully formed callus as part of the fracture healing process within three months post-fracture were classified into the normal fracture healing group (100 patients). Conversely, if no signs of healing were observed or bone atrophy occurred at the fracture ends more than three months after the fracture, it was categorized as DFH (95 patients). In such cases, a distinct fracture line is visible on X-rays, with either minimal or no callus formation.

Inclusion criteria: for patients with mature bones (aged≥18 years), the first fracture occurs, and a non-healing state has persisted for at least 3 months. X-ray examination revealed that there was no continuous callus growth at the fracture end, a distinct gap existed between the fracture ends, and the fracture end part at the fracture end showed sclerosis. Exclusion criteria: malignant tumors, incomplete cardiac, bone metabolism-related diseases, diabetes; clinical data are incomplete or missing. Table 1 collected the age, sex, factors affecting DFH (body mass index (BMI), Smoking, Alcohol intake), Fracture inducement, and basic clinical information.

Immediately after the fracture occurred in untreated subjects, 3 mL of peripheral venous blood was collected. Following coagulation, the samples were centrifuged at 3,000 rpm for 10 min. The supernatant was carefully harvested to obtain the serum. These serum samples were then stored at −80 °C until further testing.

Cell culture and transfection

The MC3T3-E1 pre-osteoblast cells were placed in the α-MEM medium and kept at a temperature of 37 °C, with 95 % air and 5 % carbon dioxide surrounding them. Subsequently, an

Table 1: Baseline clinical data of study population.

Items	NFH (n=100)	DFH (n=95)	p-Value
Age, year	49.62 ± 14.72	51.07 ± 15.15	0.497
Sex, n, (%)			0.355
Male	54 (54.00)	45 (47.37)	
Female	46 (46.00)	50 (52.63)	
BMI, kg/m^2	24.14 ± 4.23	24.54 ± 3.72	0.484
Smoking, n, (%)			0.522
Yes	37 (37.00)	31 (32.63)	
No	63 (63.00)	64 (67.37)	
Alcohol intake, n, (%)			0.887
Yes	41 (41.00)	38 (40.00)	
No	59 (59.00)	57 (60.00)	
Fracture side, n, (%)			0.893
Left	58 (58.00)	56 (58.95)	
Right	42 (42.00)	39 (41.05)	
Fracture inducement, n, (%)			0.776
Traffic injury	21 (21.00)	17 (17.89)	
Ground fall	27 (27.00)	24 (25.26)	
Spots injury	52 (52.00)	54 (56.84)	
Osteosynthesis method, n, (%)			0.874
Open reduction	61 (61.00)	59 (62.11)	
Closed reduction	39 (39.00)	36 (37.89)	

BMI, body mass index; NFH, normal fracture healing; DFH, delayed fracture healing. Independent sample Student's t-test, chi-square analysis, and one-way ANOVA, were applied as statistical methods.

osteogenic medium was added thereto, and the cultivation duration lasted for 15 days to induce cell differentiation [20].

The miR-766-3p mimics, mimics-NC, miR-inhibitor, and inhibitor-NC were synthesized by Shanghai GenePharma Co., Ltd. The concentrations of miR-766-3p mimics and miR-766-3p inhibitors were set at 50 nM. *TGFBR1* was inserted into the pcDNA3.0 expression vector (*p-TGFBR1*) to upregulate *TGFBR1* expression. When the MC3T3-E1 cells were in the logarithmic growth phase, the transfection operation was done.

RT-qPCR

Total RNA was extracted through the Trizol reagent. Then, the RNA was reverse-transcribed to obtain cDNA. Next, the expression of miR-766-3p, *TGFBR1*, RUNX2, OCN, and ALP was detected using cDNA as the template. RT-qPCR amplification was carried out through SYBR-Green PCR Master Mix (Thermo Fisher Scientific, Inc.). U6 and GAPDH were employed as internal references. The thermal cycling conditions of the PCR reaction consist of an initial template denaturation at 95 °C, along with 40 cycles of denaturation at 95 °C and annealing/extension at 60 °C. The sequences of primers were designed and obtained from Shanghai GenePharma Co., Ltd, and sequences of primers were as follow: miR-766-3p forward (5′-ACTCCAGCCCCACAGC-3′), miR-766-3p reverse (5′-GAACATGTCTGCGTATCTC-3′); TGFBR1 forward (5′-GAACTGTTTTGATTGGCATC-3′), TGFBR1 reverse (5′-AAGAAGGGACCTACACTATTT-3′); Runx2 forward (5′-TCCAGGAGGACAGCAAGGAGGC-3′), Runx2 reverse (5′-TCGGTTGGTCTCGGTGGCTGG-3′); OCN forward (5′-GCGCATCTATGGCACCACCGT-3′), OCN reverse (5′-TTTGGAGCAGCTGTGCCGTCC-3′); ALP forward (5′-GCCCAGGCAACCTCGAGCAG-3′), ALP reverse (5′-TCCGACCCACGGAGGGTTCC-3′); U6 reverse (5′-ACGCTTCACGAATTTGCGT-3′); U6 forward (5′-CTCGCTTCGGCAGCACA-3′), GAPDH forward (5′-GACAGTCAGCCGCATCTTCT-3′), GAPDH reverse (5′-GCGCCCAATACGACCAAATC-3′). Relative gene expression was quantified using the $2^{-\Delta\Delta Ct}$ method. Briefly, Ct values for both the target gene and the reference gene were recorded for each sample. For each sample, ΔCt was calculated as the difference between the Ct value of the target gene and that of the reference gene. Using the average ΔCt of the control group as a baseline, ΔΔCt was determined by subtracting the control group's ΔCt from the ΔCt of the treatment group. The relative expression level of the target gene in the treatment group, normalized to the control group, was then calculated by substituting the ΔΔCt value into the formula $2^{-\Delta\Delta Ct}$.

Cell proliferation

The CCK-8 kit (Dojindo Molecular Technologies, Inc.) was chosen to evaluate cell proliferation. Cells were seeded into 96-well plates at a density of 4×10^4 cells per well. After 0, 24, 48, and 72 h, 10 μL of CCK-8 solution was added. The cells were then incubated at 37 °C for 30 min. The absorbance was measured at 450 nm.

Analysis of apoptosis

Flow cytometry detection was performed according to the instructions of the Annexin V/propidium iodide (PI) kit. The transfected cells were collected in a centrifuge tube for centrifugation, then suspended and washed with PBS, and centrifuged again. Subsequently, Annexin V/FITC was added and suspended in the dark. Thereafter, PI and PBS were added, and the flow cytometry was utilized to detect apoptotic cells. The final count of apoptotic cells was quantified as the combined percentage of early apoptotic cells (staining positive for Annexin V and negative for PI) and late apoptotic cells (positive for both Annexin V and PI). The cell apoptosis rate was calculated using the following formula: Cell Apoptosis Rate (%) = (Number of Apoptotic Cells/Total Number of Cells) × 100, ensuring precise quantification of cellular apoptotic activity.

Enzyme-linked immunosorbent assay (ELISA)

For the determination of the content of tumor necrosis factor-alpha (TNF-α) and interleukin-6 (IL-6) in MC3T3-E1 cells, the specific procedures were as follows: Cells at the logarithmic growth phase were implanted in a 6-well plate and triggered for cultured for 7 days. Subsequently, the cell supernatant was collected, and the expressions of TNF-α and IL-6 were measured strictly per the operation instructions provided by the ELISA kit (TNF-α: Human TNF alpha ELISA Kit, KHC3014, intra-assay % CV: 5.9 %, inter-assay % CV: 8.5 %; IL-6: Human IL-6 ELISA Kit, BMS213-2, intra-assay % CV: 3.4 %, inter-assay % CV: 5.2 %. Invitrogen Inc Thermo Fisher.).

Luciferase report assay

The primers for the 3′-UTR of the *TGFBR1* gene were designed using Primer Premier 5.0 and subsequently amplified by PCR. The resulting PCR product was cloned into the pGLO plasmid (Promega, USA) to construct the

wild-type *TGFBR1* vector (WT-*TGFBR1*). Furthermore, site-directed mutagenesis was performed on the 3′-UTR sequence of *TGFBR1* to generate the mutant vector (MUT-*TGFBR1*). Subsequently, they were mixed with the miR-766-3p mimics, inhibitors, or their negative control for co-transfection. Forty-eight hours later, the luciferase activity was detected.

Statistical analysis

Statistical analysis was performed using SPSS 22.0 and GraphPad Prism 9.0. Data normality was initially evaluated using the Kolmogorov–Smirnov (K-S) test to determine the appropriateness of parametric statistical methods. For continuous variables that failed to meet normality assumptions, intergroup differences between two groups were analyzed using the non-parametric Mann–Whitney U test. Conversely, a Student's t-test was applied to compare data between the two groups. Categorical variables were assessed using the chi-square test. One-way ANOVA was used to perform multiple comparisons among groups. The ROC curve was employed to assess the predictive value. COX regression was conducted to identify potential independent risk factors of DFH. Each cellular experiment was repeated three times. When $p<0.05$, it was regarded as statistically significant.

Results

miR-766-3p has a strong discriminatory ability in predicting DFH

There was no significant association between normal fracture-healing patients and DFH patients in terms of age, sex, BMI, smoking, drinking, fracture side, fracture inducement, and osteosynthesis method (Table 1). The expression of miR-766-3p of DFH was significantly lower (Figure 1A). The ROC result revealed that the area under the curve (AUC) of miR-766-3p was 0.936 (95 % CI: 0.8988–0.9723), the specificity was 80.0 %, and the sensitivity was 96.8 %, suggesting that miR-766-3p has a strong discriminatory ability in predicting DFH (Figure 1B). COX regression analysis demonstrated that miR-766-3p served as an independent predictive factor influencing DFH (Table 2). Thus, miR-766-3p may be related to the DFH.

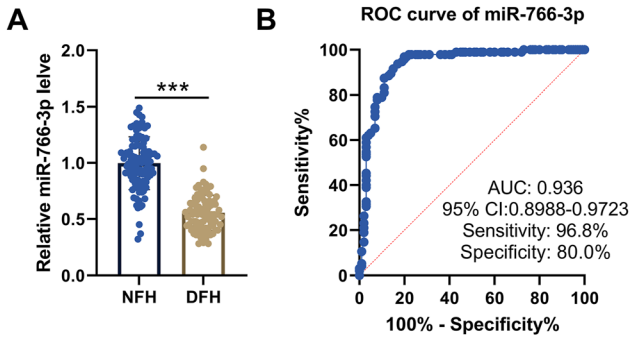

Figure 1: **A**. Comparison of serum miR-766-3p expression between the two groups. *** means p<0.001. **B**. ROC curve for evaluating the clinical diagnostic. Non-parametric tests and ROC curves were employed as statistical methods.

Table 2: Cox regression analysis of independent risk indicators for patients with DFH.

Items	HR	95 % CI	p-Value
Age, year	1.161	0.775–1.739	0.470
Sex	1.028	0.687–1.539	0.893
BMI, kg/m^2	1.224	0.816–1.836	0.328
Smoking,	1.119	0.729–1.720	0.607
Alcohol intake	1.119	0.742–1.689	0.591
Fracture side	1.159	0.767–1.751	0.484
Fracture inducement			0.909
Traffic injury	–	–	–
Ground fall	0.969	0.519–1.808	0.921
Spots injury	1.072	0.621–1.852	0.802
Osteosynthesis method	1.149	0.758–1.741	0.513
miR-766-3p expression	0.074	0.032–0.169	<0.001[a]

BMI, body mass index; DFH, delayed fracture healing; HR, Hazard Ratio; CI, confidence interval. [a]means p<0.001. Logistic regression analysis was applied as a statistical method.

Impact of miR-766-3p on osteogenic differentiation and inflammatory microenvironment

With the prolongation of osteogenic induction time, the expression of osteogenic markers RUNX2, OCN, and ALP gradually increased, and the cells were successfully differentiated (Figure 2A). The expression of miR-766-3p gradually increased (Figure 2B). Subsequently, the expression of miR-766-3p was significantly increased or inhibited by transfection of miR-mimic or miR-inhibitor (Figure 2C). Overexpression of miR-766-3p could significantly promote the proliferation (Figure 2D). In addition, an increase in miR-766-3p could significantly promote the differentiation of

osteogenic markers ALP, OCN, and RUNX2 (Figure 2E), inhibit cell apoptosis (Figure 2F), reduce the expression of TNF-α and IL-6 (Figure 2G), while inhibition of miR-766-3p exhibited the opposite phenomenon.

miR-766-3p targeted and regulated TGFBR1

The database showed that *TGFBR1* was a downstream regulatory gene of miR-766-3p (Figure 3A). miR-766-3p mimic significantly inhibited the luciferase activity of the WT-*TGFBR1* group, but did not affect the MUT-*TGFBR1* group (Figure 3B). *TGFBR1* decreased with the prolongation of the osteogenic induction time (Figure 3C). There was a significant negative association between miR-766-3p and *TGFBR1* expression (Figure 3D).

Overexpression of TGFBR1 reversed the effect of miR-766-3p on cell behavior

To further explore the regulatory mechanism of miR-766-3p and *TGFBR1* in DFH, during the overexpression of miR-766-3p, miR-mimic+p-*TGFBR1* was co-transfected (Figure 4A). The results indicated that the increase of *TGFBR1* inhibited the cell proliferation induced by miR-766-3p (Figure 4B). Simultaneously, the elevated *TGFBR1* suppressed osteoblast biomarkers ALP, OCN, and RUNX2 expressions (Figure 4C). Regarding cell apoptosis and inflammatory response, the increased *TGFBR1* promoted cell apoptosis (Figure 4D) and also facilitated the occurrence of inflammation (Figure 4E).

Discussion

Following a fracture, the blood circulation is compromised, and the prognosis after surgery is often delayed [21]. MiRNAs play a crucial role in inflammatory diseases and neurological disorders [14]. For instance, miR-181a-5p is implicated in DFH [22], and miR-31-5p is specifically regulated in nonunion fractures [23]. Studies have demonstrated that overexpression of miR-766-3p can inhibit chondrocyte apoptosis [14] and is positively correlated with the bone mineral density (BMD) value in osteoporosis patients [13]. Nevertheless, the function of miR-766-3p in the course of DFH remains to be undefined.

Our study involving 100 patients with normal fracture healing and 95 DFH patients revealed that the serum miR-766-3p in DFH was greatly decreased. miR-766-3p exhibited a robust predictive capacity for DFH and may serve as a potential risk factor for its development. Osteoblasts play a crucial role in the growth of normal bone tissue. The loss of their function may result in DFH [22]. Our research has revealed that miR-766-3p would increase with

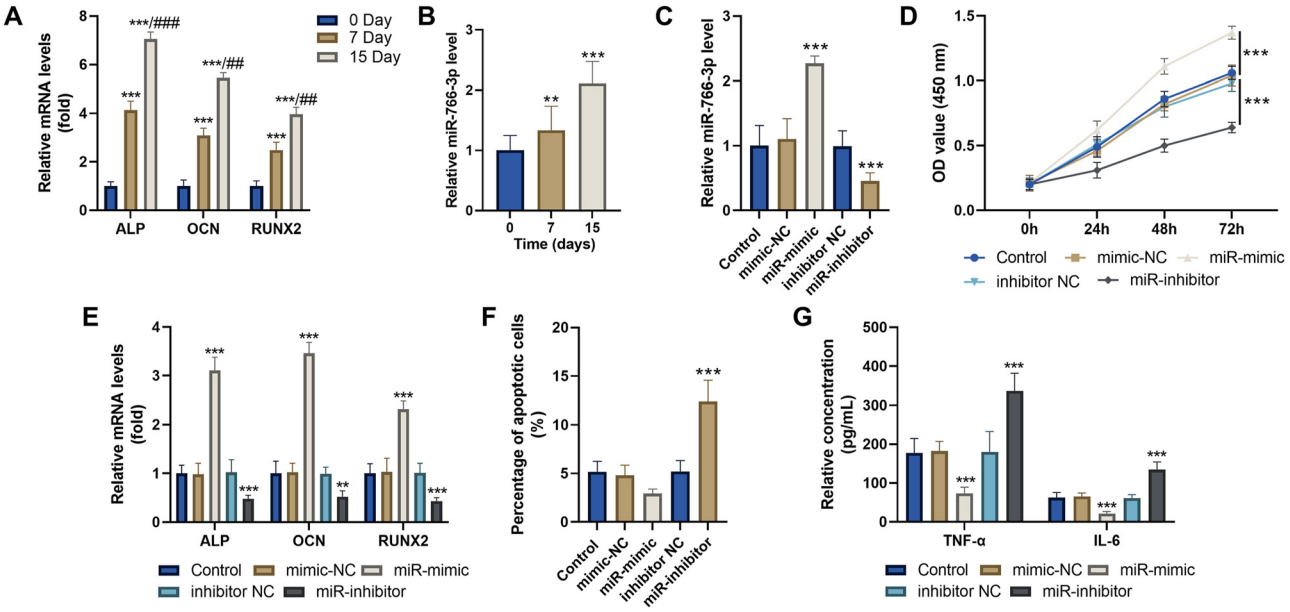

Figure 2: Cell function experiments were carried out on the MC3T3-E1 cell line (n=5). **A**. Changes in the proteins of cell differentiation markers. **B**. After inducing the differentiation of cells, miR-766-3p was increased. **C**. RT-qPCR for evaluating transfection efficiency. **D**. CCK-8 experiment. **E**. The mRNA expression of cell differentiation marker proteins. **F**. Flow cytometry for detecting apoptosis. **G**. ELISA for detecting the expression of inflammatory factors. *** means p<0.001 compared to the control group. Non-parametric tests were employed as statistical methods.

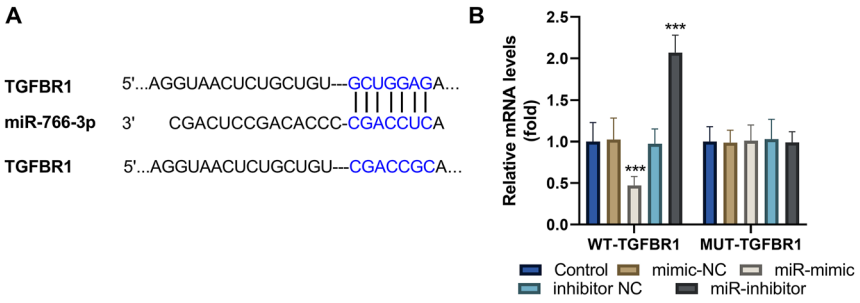

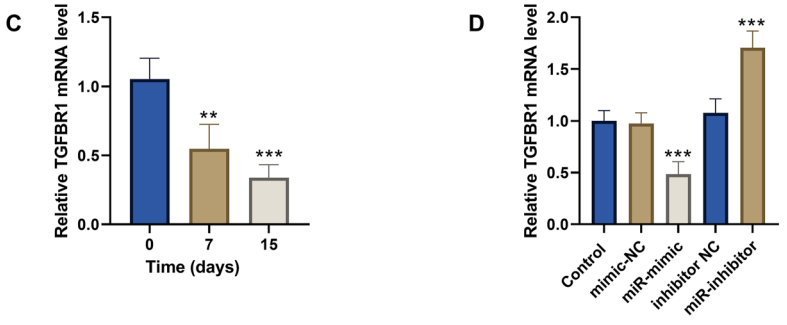

Figure 3: Target gene prediction. **A**. The targeting sequence between miR-766-3p and *TGFBR1*. **B**. The dual-luciferase reporter assay was employed to verify the interaction between miR-766-3p and *TGFBR1*. **C**. RT-qPCR for detecting the expression change of *TGFBR1* after inducing the differentiation of MC3T3-E1 cells. **D**. The expression of *TGFBR1* in cells. ** means p<0.01, *** means p<0.001. Non-parametric tests were employed as statistical methods.

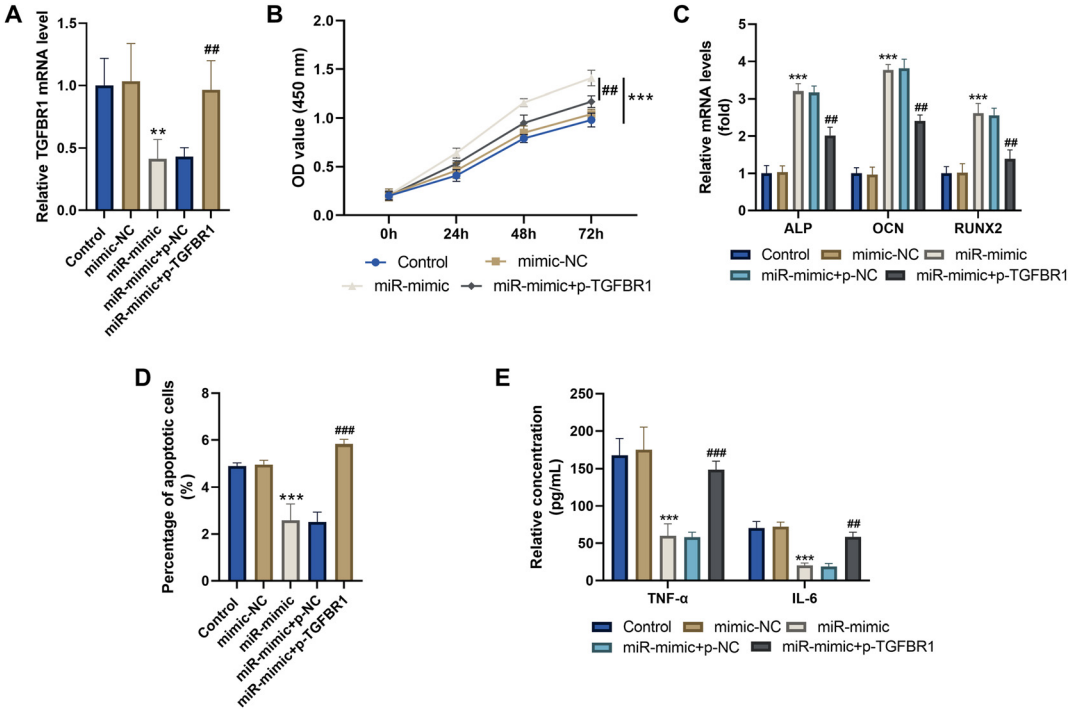

Figure 4: In the MC3T3-E1 cell line, miR-766-3p and *TGFBR1* were co-regulated (n=5). **A**. The mRNA expression of *TGFBR1* in the MC3T3-E1 cell line. **B**. CCK-8 experiment. **C**. The mRNA expression of cell differentiation marker proteins. **D**. Flow cytometry for detecting apoptosis. E. ELISA was employed to detect the expression of inflammatory factors. ** means p<0.01, *** means p<0.001 relative to control group; ## means p<0.01, ### means p<0.001 relative to miR-mimic group. Non-parametric tests were employed as statistical methods.

the increase of osteogenic differentiation time. Overexpression of miR-766-3p could significantly promote proliferation and differentiation while inhibiting apoptosis and inflammatory response. miR-766-3p may serve as a potential predictor and functional regulator in DFH. Its downregulation may contribute to delayed fracture healing by

suppressing osteoblast activity, enhancing apoptosis, and exacerbating inflammatory responses.

TGFBR1 exerts a negative regulatory effect on bone formation and plays a crucial role in the osteogenic differentiation of mouse bone marrow mesenchymal stem cells [17, 19]. Our research verified that miR-766-3p targeted and negatively regulated *TGFBR1*. Regarding cell function, we found that *TGFBR1* overexpression significantly abolished the promoting effect of miR-766-3p on the differentiation and proliferation of MC3T3-E1 osteoblasts, as well as the inhibitory effect on cell apoptosis and inflammatory response. This suggested that miR-766-3p regulated osteoblast function by directly targeting *TGFBR1*. An imbalance in the expression of miR-766-3p and *TGFBR1* could potentially result in abnormal osteoblast function, consequently impacting the fracture healing process and contributing significantly to the pathogenesis and progression of DFH. Clinically, regularly monitoring the expression changes of miR-766-3p and *TGFBR1* may serve as a potential approach to predict the risk of DFH in advance, thereby enabling timely intervention measures.

In addition, this study had certain limitations that warrant acknowledgment. First, the relatively small sample size and lack of ethnic diversity may compromise the representativeness and generalizability of the findings. Second, the absence of supporting animal experimental data limits the mechanistic insights into the roles of miR-766-3p and *TGFBR1*. Future studies should aim to enhance external validity by increasing the sample size and recruiting a more ethnically diverse population. At the same time, relevant animal experiments will be carried out to systematically explore the effects of miR-766-3p and *TGFBR1* on DFH.

In brief, miR-766-3p typically promoted the differentiation and proliferation of osteoblast MC3T3-E1 and inhibited cell apoptosis. Nevertheless, these effects of miR-766-3p can be significantly nullified by *TGFBR1* overexpression. This might be the potential mechanism resulting in DFH. Our findings contributed to understanding the mechanism of delayed healing of DFH.

Research ethics: This study was approved by the Cangxian Hospital Ethics Committee (approval number: 2021003, Date: 2021.01.11). All procedures adhere to the Helsinki Declaration.

Informed consent: The subjects signed the informed consent form.

Author contributions: GRZ and LCL made substantial contributions to conception and design, performed all the experiment, and was a major contributor in writing the manuscript. PJL and JHR contributed to acquisition of patients and tissues specimens, analysis and interpretation of data. YR has been involved in drafting the manuscript and revising it critically for important intellectual content.

Use of Large Language Models, AI and Machine Learning Tools: Not applicable.

Conflict of interest: The author states no conflict of interest.

Research funding: None declared.

Data availability: The datasets used and/or analyzed during the current study are available from the corresponding author upon reasonable request.

References

1. Zhang X, Chen Y, Zhang C, Zhang X, Xia T, Han J, et al. Effects of icariin on the fracture healing in young and old rats and its mechanism. Pharm Biol 2021;59:1245–55.
2. Xu B, Anderson DB, Park ES, Chen L, Lee JH. The influence of smoking and alcohol on bone healing: systematic review and meta-analysis of non-pathological fractures. eClinicalMedicine 2021;42:101179.
3. Chitwood JR, Chakraborty N, Hammamieh R, Moe SM, Chen NX, Kacena MA, et al. Predicting fracture healing with blood biomarkers: the potential to assess patient risk of fracture nonunion. 2021;26(8): 703-17.
4. Zhou QP, Zhang F, Zhang J, Ma D. H19 promotes the proliferation of osteocytes by inhibiting p53 during fracture healing. Eur Rev Med Pharmacol Sci 2018;22:2226–32.
5. Zhang Y, Yuan Q, Wei Q, Li P, Zhuang Z, Li J, et al. Long noncoding RNA XIST modulates microRNA-135/CREB1 axis to influence osteogenic differentiation of osteoblast-like cells in mice with tibial fracture healing. Hum Cell 2022;35:133–49.
6. Filipowicz W, Bhattacharyya SN, Sonenberg N. Mechanisms of post-transcriptional regulation by microRNAs: are the answers in sight? Nat Rev Genet 2008;9:102–14.
7. Kuehbacher A, Urbich C, Zeiher AM, Dimmeler S. Role of Dicer and Drosha for endothelial microRNA expression and angiogenesis. Circ Res 2007;101:59–68.
8. Suarez Y, Fernandez-Hernando C, Pober JS, Sessa WC. Dicer dependent microRNAs regulate gene expression and functions in human endothelial cells. Circ Res 2007;100:1164–73.
9. Lei SF, Papasian CJ, Deng HW. Polymorphisms in predicted miRNA binding sites and osteoporosis. J Bone Miner Res 2011;26:72–8.
10. Seeliger C, Karpinski K, Haug AT, Vester H, Schmitt A, Bauer JS, et al. Five freely circulating miRNAs and bone tissue miRNAs are associated with osteoporotic fractures. J Bone Miner Res 2014;29:1718–28.
11. Zhou L, Zhang X, Wang Z, Li D, Zhou G, Liu H, et al. Extracellular vesicle-mediated delivery of miR-766-3p from bone marrow stromal cells as a therapeutic strategy against colorectal cancer. Cancer Cell Int 2024;24: 330.
12. Cui S, Zhou Z, Liu X, Richards RG, Alini M, Peng S, et al. Identification and characterization of serum microRNAs as biomarkers for human disc degeneration: an RNA sequencing analysis. Diagnostics 2020;10. https://doi.org/10.3390/diagnostics10121063.
13. Shi H, Jiang X, Xu C, Cheng Q. MicroRNAs in serum exosomes as circulating biomarkers for postmenopausal osteoporosis. Front Endocrinol 2022;13:819056.
14. Li Z, Cheng J, Liu J. Baicalin protects human OA chondrocytes against IL-1beta-induced apoptosis and ECM degradation by activating

autophagy via MiR-766-3p/AIFM1 Axis. Drug Des Dev Ther 2020;14: 2645–55.
15. Hayakawa K, Kawasaki M, Hirai T, Yoshida Y, Tsushima H, Fujishiro M, et al. MicroRNA-766-3p contributes to anti-inflammatory responses through the indirect inhibition of NF-kappaB signaling. Int J Mol Sci 2019;20:809.
16. Rahman MS, Akhtar N, Jamil HM, Banik RS, Asaduzzaman SM. TGF-β/BMP signaling and other molecular events: regulation of osteoblastogenesis and bone formation. Bone research 2015;3:15005.
17. Shen GY, Ren H, Shang Q, Zhao WH, Zhang ZD, Yu X, et al. Let-7f-5p regulates TGFBR1 in glucocorticoid-inhibited osteoblast differentiation and ameliorates glucocorticoid-induced bone loss. Int J Biol Sci 2019;15: 2182–97.
18. Luo D, Xie W, He X, Zhou X, Ye P, Wang P, et al. Exosomal miR-590-3p derived from bone marrow mesenchymal stem cells promotes osteoblast differentiation and osteogenesis by targeting TGFBR1. Vitro Anim Cell Dev Biol 2025;61:46–58.
19. Maeda S, Hayashi M, Komiya S, Imamura T, Miyazono K. Endogenous TGF-beta signaling suppresses maturation of osteoblastic mesenchymal cells. EMBO J 2004;23:552–63.
20. Gong K, Qu B, Liao D, Liu D, Wang C, Zhou J, et al. MiR-132 regulates osteogenic differentiation via downregulating Sirtuin1 in a peroxisome proliferator-activated receptor beta/delta-dependent manner. Biochem Biophys Res Commun 2016;478:260–7.
21. Clement ND, Gaston MS, Simpson AH. Fractures in elderly mice demonstrate delayed ossification of the soft callus: a cellular and radiographic study. Eur J Orthop Surg Traumatol 2023;33:977–85.
22. Guo X, Zhang J, Han X, Wang G. LncRNA SNHG1 delayed fracture healing via modulating miR-181a-5p/PTEN Axis. J Invest Surg 2022;35: 1304–12.
23. Breulmann FL, Hatt LP, Schmitz B, Wehrle E, Richards RG, Della BE, et al. Prognostic and therapeutic potential of microRNAs for fracture healing processes and non-union fractures: a systematic review. Clin Transl Med 2023;13:e1161.